

Catalytic Performance of Oxidized Ni₃Sn₂ for Hydrogen Production from Methanol Decomposition

Pan Wei, Lingtong Zhou, Wei Xia, Zhujian Li, Haifei Long,
Jindan Chen, Ting Li and Mei Qiang Fan*

Department of Materials Science and Engineering, China Jiliang University, Hangzhou 310018, P R China

Received: March 03, 2014, Accepted: July 16, 2014, Available online: August 13, 2014

Abstract: The catalytic properties of oxidized Ni₃Sn₂ powders were investigated for producing hydrogen from decomposing methanol in the temperatures ranging from 240 to 480 °C. The oxidized Ni₃Sn₂ had much higher catalytic activity than that of Ni₃Sn₂ in the temperature range of 320~400 °C. The results of an isothermal test performed at 320 °C revealed that the oxidized Ni₃Sn₂ was spontaneously activated within 4 h of the reaction and slowly deactivated in the followed reaction time. The oxidized Ni₃Sn₂ suppressed side reactions such as methanation and water-gas shift reaction and showed a high efficiency for H₂ production from methanol decomposition. Surface analysis revealed that the activity of oxidized Ni₃Sn₂ was attributed to the formation of Ni/SnO₂ catalyst, which was supposed to serve as active sites for methanol decomposition.

Keywords: Methanol decomposition; hydrogen production; catalytic activity; Ni/Sn oxides

1. INTRODUCTION

Ni-Sn intermetallic compounds (IMCs) have the potential to show high catalytic activity, high selectivity to desired products, and high durability due to the positive effects arising from the cooperative interaction between Ni and Sn.¹⁻³⁾ It was reported that the addition of Sn to Ni decreases the rate of methane formation from C-O bond cleavage, while maintaining high rates of C-C cleavage required for hydrogen formation.⁴⁻⁶⁾ Ni-Sn IMCs were expected to play an important role in Ni-Sn catalysts for hydrogen production. Dumesic [5] reported that the addition of Sn to Ni improved the selectivity for hydrogen production by ethylene glycol reforming and evidence for the formation of Ni₃Sn alloy associated with alumina was obtained by Mossbauer spectroscopy. Onda et al.[6] studied the catalytic properties of Ni₃Sn, Ni₃Sn₂, and Ni₃Sn₄ for the partial hydrogenation of acetylene into ethylene and reported that the high degrees of selectivity of Ni₃Sn and Ni₃Sn₂ were attributed to the Sn-induced decrease in catalytic activity. For practical use, it was a potential requirement for developing a high-activity and cheap catalyst and lowering the activation temperature for hydrogen production.

In this study, we performed the methanol decomposition over

oxidized Ni₃Sn₂ single-phase powders to evaluate their catalytic properties for hydrogen production. The microstructure of the powder surface was investigated before and after reaction in order to understand the catalytic behavior of oxidized Ni₃Sn₂. Our attempt was to improve the activity of Ni₃Sn₂ IMC and explore an effective method for catalyst preparation.

2. EXPERIMENTAL

2.1. Sample preparation

Ni₃Sn₂ ingots were prepared by melting the mixture of stoichiometric amounts of nickel and tin metals in a high-frequency vacuum melting furnace. Ingots thus obtained were crushed in air and filtered into particles with diameters between 25~75 μm. The oxidation of Ni₃Sn₂ powder was performed in Muffle furnace at air for 5 h. The heating rate was defined to 10 °C/min and the oxidation temperatures were set to 900 and 1100 °C.

2.2. Catalytic activity measurement

Catalytic activity experiments were performed in a conventional fixed-bed flow reactor. The reactor was made of a quartz tube with an internal diameter of 8 mm and the catalyst weight was 0.4 g. The catalyst was used without any handling. The methanol was introduced in a flow rate of 100 μl/min and the liquid hourly space

*To whom correspondence should be addressed: Email: fanmeiqiang@126.com
Phone:

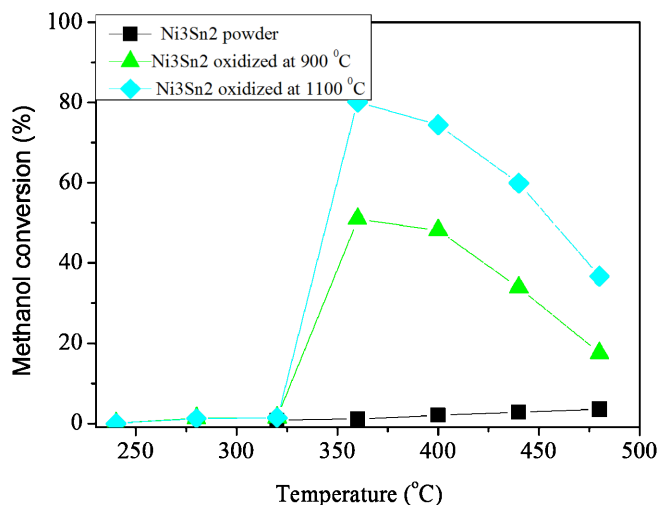


Figure 1. shows the conversion of methanol over the oxidized Ni₃Sn₂ powders plotted as functions of decomposition temperature during the isochronal test.

velocity (LHSV) of methanol was calculated to be approximately 70 h⁻¹ (defined as the volume of methanol passed over the unit volume of catalyst per hour).

The catalytic activity measurement includes isochronal and isothermal tests. The isochronal test was carried out with increasing reaction temperature stepwise from 240 to 480 °C at an interval of 40 °C. The outlet composition and total flow rate of the gaseous products were collected after holding at each temperature for 20 min. The isothermal test was carried out at 320 °C for 28 h, and the outlet composition and total flow rate of the gaseous products were collected during reaction.

2.3. Catalyst characterization

The crystal structures of Ni₃Sn₂ before and after oxidation were characterized by an X-ray diffractometer (Thermo ARL, Switzerland, model ARL X'TRA) using a CuK α source. The surface morphology and the composition of the samples were examined using JSM-5610LV model (JEOL Company) equipped with INCA energy dispersive X-ray spectroscopy (EDS) measurements. The Brunauer-Emmett-Teller (BET) surface area was determined with a surface area analyzer (Micromeritics, ASAP2020/ Tristar 3000) using N₂ as adsorbents.

3. RESULTS AND DISCUSSION

3.1. Catalysis activity

Figure 1 shows the conversion of methanol over the oxidized Ni₃Sn₂ powders plotted as functions of decomposition temperature during the isochronal test. Ni₃Sn₂ had slow increase of methanol conversion with increasing temperature and it had below 3.5 % of methanol conversion even at 480 °C and. In contrast, the oxidized Ni₃Sn₂ exhibited different evolution trend of methanol conversion with increasing temperature. There was below 1% of methanol conversion over oxidized Ni₃Sn₂ powders below 320 °C. The oxidized Ni₃Sn₂ powders rapidly increased the conversion of methanol with increasing decomposition temperature above 320 °C, and the

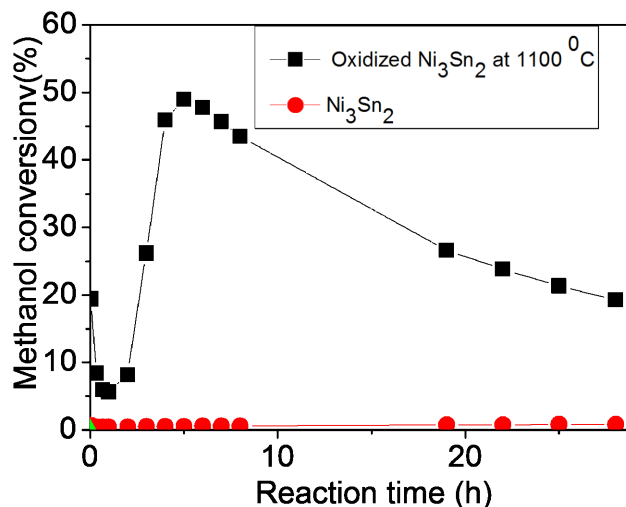


Figure 2. shows the conversion of methanol over Ni₃Sn₂ and oxidized Ni₃Sn₂ powders at 320 °C plotted as functions of decomposition time.

largest value of the methanol conversion was obtained at 360 °C, then the methanol conversion was subsequently decreased with increasing temperature. It was also observed that the largest value of methanol conversion over oxidized Ni₃Sn₂ powders at 360 °C was significantly affected by oxidation temperature. The largest value of methanol conversion over oxidized Ni₃Sn₂ at 900 and 1100 °C was corresponded to 51 and 80%, respectively. Higher oxidation temperature of Ni₃Sn₂ led to higher methanol conversion during the reaction. These results indicate that oxidized Ni₃Sn₂ shows much higher catalytic activity than Ni₃Sn₂, especially at 360 °C.

The isothermal test was performed on the catalysts at 320 °C for 28 h to examine the catalytic properties in more detail. Figure 2 shows the conversion of methanol over Ni₃Sn₂ and oxidized Ni₃Sn₂ powders at 320 °C plotted as functions of decomposition time. Below 1% of the methanol was converted over Ni₃Sn₂ within 28 h of reaction, reflected that there was almost no activity over Ni₃Sn₂ below 320 °C. About 20% of the methanol was converted over Ni₃Sn₂ oxidized at 1100 °C when the test started. Interestingly, the conversion of methanol significantly decreased from 0 to 1 h, increased from 1 to 5 h, then decreased irreversibly from 5 to 28 h. 49% of the largest methanol conversion was obtained after 5 h and approximate 19% of the methanol was still converted after 28 h. These results reveal that oxidized Ni₃Sn₂ was spontaneously activated during the period of 0~5 h and deactivated in the range of 5~28 h. It was clearly observed that the deactivation of oxidized Ni₃Sn₂ became slower with increasing methanol decomposition time from Figure 2, showed that oxidized Ni₃Sn₂ still had much high activity than that of Ni₃Sn₂ after long reaction time.

Figure 3 plots the rates at which H₂, CO, CH₄, H₂O, and CO₂ were produced over oxidized Ni₃Sn₂ at 320 °C as functions of methanol decomposition time. The production rates of H₂ and CO were much higher than those of the other gases, and the ratio of the H₂ to CO produced (H₂/CO) was close to 2, which is stoichiometric for methanol decomposition, indicating that the methanol had mainly

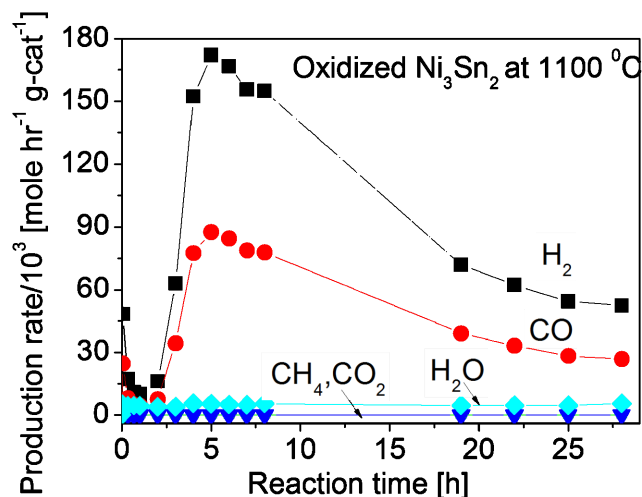
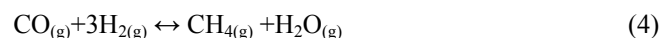
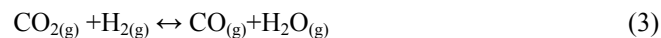


Figure 3. plots the rates at which H₂, CO, CH₄, H₂O, and CO₂ were produced over oxidized Ni₃Sn₂ at 320 °C as functions of methanol decomposition time.

decomposed according to the following reaction (Eq. 1). The production rate of H₂ and CO was still up to 52.4 and 26.6 × 10⁻³ mole hr⁻¹ g-cat⁻¹ after 28 h of reaction, respectively.



The production rates of CH₄ and CO₂ were 0 and the production rate of H₂O was kept at approximate 5 × 10⁻³ mole hr⁻¹ g-cat⁻¹ within 28 h of reaction, reflected that there were a little Boudouard reaction (Eq. 2), reverse water-gas shift reaction (Eq. 3) but no methanation (Eq. 4) during the reaction at 320 °C.



3.2. Surface characterization of Ni₃Sn₂ before and after oxidation

Figure 4 shows XRD patterns obtained for Ni₃Sn₂ before and after oxidation at 900 and 1100 °C. The initial XRD patterns were obtained using Ni₃Sn₂ powders before oxidation and only show diffraction peaks attributed to Ni₃Sn₂ (Orthorhombic, Pnma), indicating that the Ni₃Sn₂ samples consisted of pure single-phase powders. The XRD patterns obtained for Ni₃Sn₂ after oxidation were completely different to the initial XRD patterns, and they showed some peaks attributable to other phases such as oxides of Ni or Sn, suggesting that the Ni₃Sn₂ were completely oxidized in air at above 900 °C. Some diffraction peaks attributable to NiO and SnO₂ were identified in the XRD pattern obtained for oxidized Ni₃Sn₂ and the peaks became stronger with increasing oxidation temperature. There were other peaks at 28.7°, 42.7°, 45.1° and 55.5° identified to be those of NiSnO₃ in the XRD patterns of oxidized Ni₃Sn₂ at 900 °C and they disappeared in the XRD patterns of oxidized Ni₃Sn₂ at 1100 °C.

The surface morphologies of Ni₃Sn₂ before and after oxidation

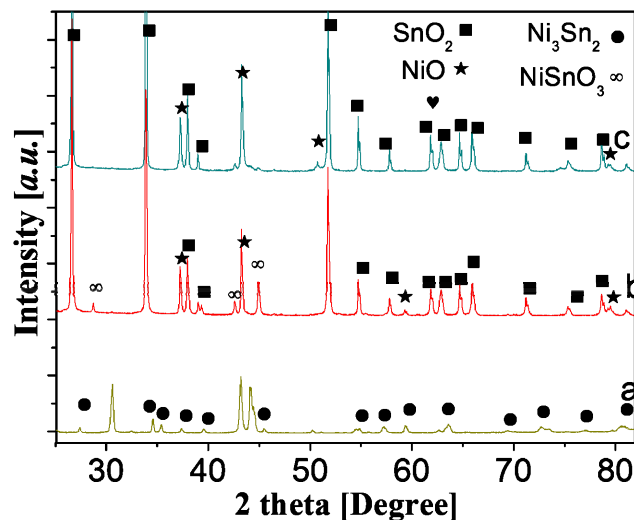


Figure 4. shows XRD patterns obtained for Ni₃Sn₂ before (a) and after oxidation at 900(b) and 1100 °C (c).

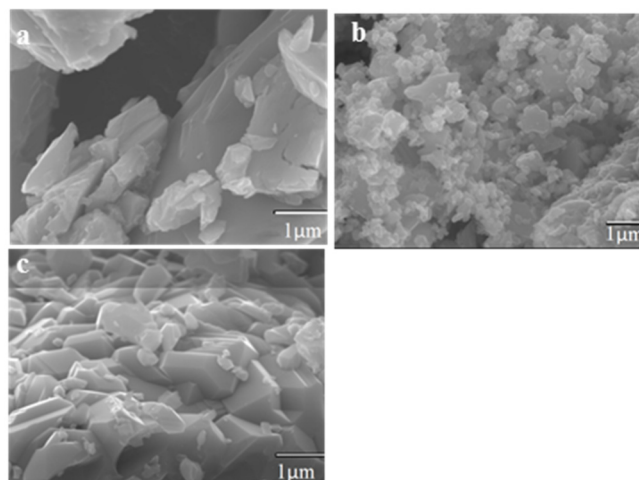


Figure 5. SEM images of Ni₃Sn₂ surfaces before (a) and after oxidation at 900 (b) and 1100 °C (c).

were analyzed using SEM and the results are shown in Figure 5. Ni₃Sn₂ showed relatively smooth surfaces with a few small particles, several hundreds of nm in diameter, before oxidation. The surfaces changed significantly after oxidation. Many small particles ranging in hundreds of nm were observed on the surface of Ni₃Sn₂ oxidized at 900 °C. The small particles presented loose and irregular structure. With increasing oxidation temperature from 900 to 1100 °C, the small particles sintered together and their size became larger. The morphology of the particles changed from irregular to regular shape such as hexagon diamond, which was the crystal structure of NiO and SnO₂.

The specific BET surface areas of the Ni₃Sn₂ particle were measured before and after oxidation and the results are shown in Table 1. The Ni₃Sn₂ particle showed very small specific surface areas (<0.1 m²/g) before oxidation. After oxidation at 900 °C, the Ni₃Sn₂

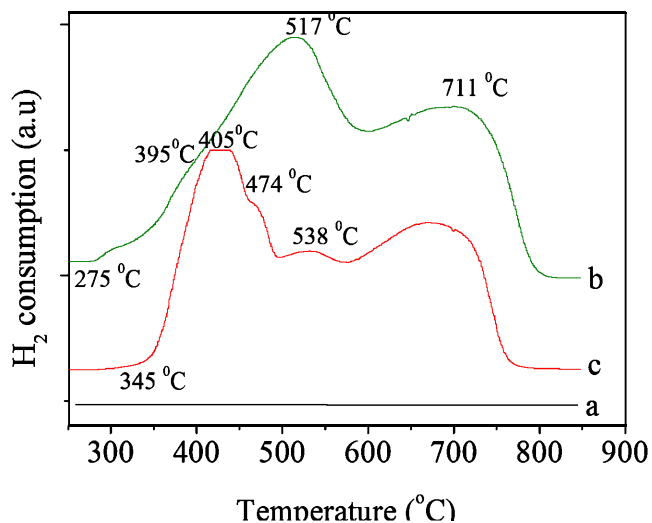


Figure 6. TPR profiles of Ni_3Sn_2 powders before (a) and after oxidation at 900 (b) and 1100 °C (c).

-particle surface area increased to $1.41 \text{ m}^2/\text{g}$, ~ 20 times larger than its initial surface area before oxidation. After oxidation at 1100 °C, the Ni_3Sn_2 -particle surface area was corresponded to $0.53 \text{ m}^2/\text{g}$, which was only one-third than that after oxidation at 900 °C.

3.3. TPR results of oxidized Ni_3Sn_2

Figure 6 shows TPR profiles of Ni_3Sn_2 before and after oxidation at 900 and 1100 °C. There was no reduction of intermetallic compound Ni_3Sn_2 while several reduction peaks were observed for oxidized Ni_3Sn_2 . The peaks were corresponded to the reduction of $\text{NiO} \rightarrow \text{Ni}$ [7], $\text{SnO}_2 \rightarrow \text{SnO}$ [8], $\text{SnO} \rightarrow \text{Sn}$ [8] and $\text{NiSnO}_3 \rightarrow \text{Ni} + \text{SnO}$. The reduction peaks had some changes except those of $\text{SnO} \rightarrow \text{Sn}$ at 717 °C with increasing oxidation temperature. The reduction peak of $\text{NiO} \rightarrow \text{Ni}$ was slightly shifted to low temperature from 405 to 395 °C and its starting reduction temperature was significantly reduced from 345 to 275 °C with increasing oxidation temperature from 900 to 1100 °C. The reduction peak at 538 °C was corresponded to that of $\text{NiSnO}_3 \rightarrow \text{Ni} + \text{SnO}$. The peak was shifted to high temperature, became weaker and finally disappeared with increasing oxidation temperature. It might be due to the decomposition of NiSnO_3 at high temperature. The reduction peak of $\text{SnO}_2 \rightarrow \text{SnO}$ at 474 °C appeared on TPR curves for the Ni_3Sn_2 oxidized at 900 °C and the peak became stronger with increasing oxidation temperature. The reduction temperature of $\text{SnO}_2 \rightarrow \text{SnO}$ was also shifted to high temperature with increasing oxidation temperature, which may be related to the sintering effect.

Table 1. BET surface areas (m^2/g) of Ni_3Sn_2 before (a) and after oxidation at 900 and 1100 °C.

Samples	Specific surface area (m^2/g)
Ni_3Sn_2 powder	0.06
Oxidized Ni_3Sn_2 powder at 900 °C in air for 5 h	1.41
Oxidized Ni_3Sn_2 powder at 1100 °C in air for 5 h	0.53

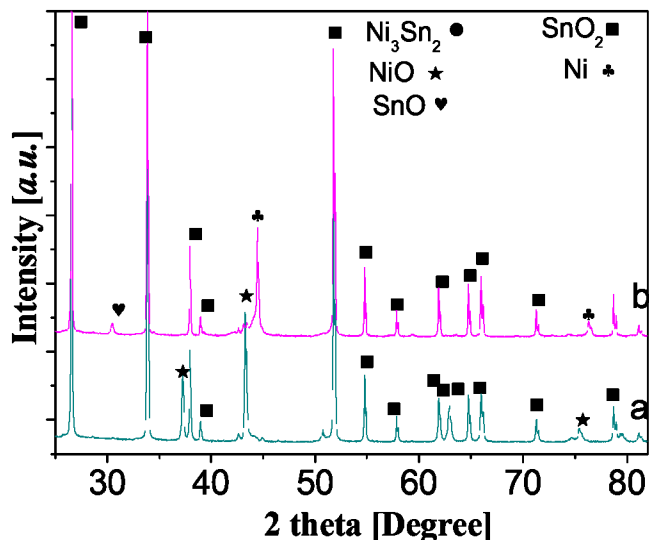


Figure 7. shows XRD patterns obtained for oxidized Ni_3Sn_2 at 1100 °C before (a) and after isothermal test (b) at 320 °C.

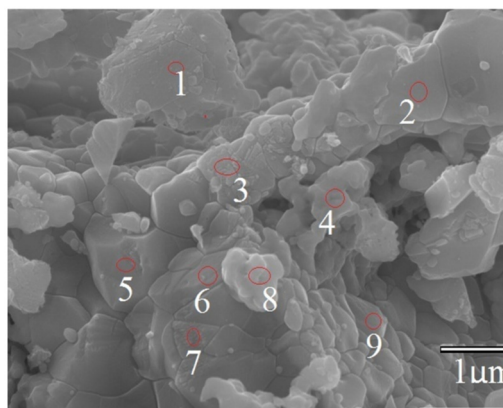


Figure 8. SEM images of oxidized Ni_3Sn_2 after 28 h of reaction at 320 °C. The used samples was oxidized at 1100 °C.

3.4. Surface characterization of oxidized Ni_3Sn_2 after isothermal test

Figure 7 shows XRD patterns obtained for oxidized Ni_3Sn_2 at 1100 °C before and after isothermal test at 320 °C. Before reaction, the peaks of NiO and SnO_2 were identified in the XRD patterns of oxidized Ni_3Sn_2 at 1100 °C. After reaction at 320 °C, the peaks of NiO disappeared due to the reduction of NiO and the result was in agreement with TPR results. The peaks of Ni and SnO_2 were identified and dominated, reflected that Ni and SnO_2 were main products of oxidized Ni_3Sn_2 after reaction. There was a weak peak of SnO observed, which was explained from the partial reduction of SnO_2 in methanol decomposition [9].

The surface morphologies of the oxidized Ni_3Sn_2 after reaction were further analyzed using SEM equipped with EDS and the results are shown in Figure 8 and table 2. The morphology had a few changes and the hexagon diamond of oxidized Ni_3Sn_2 at 1100 °C disappeared after methanol decomposition. The size of some parti-

cles became large due to the caking in methanol decomposition. Some porous structures over the surfaces were observed and they might be formed due to the loss of oxygen from the reduction of NiO→Ni. Interestingly, the carbon fiber or graphite was not easily observed on the surface of oxidized Ni₃Sn₂ after 28 h of reaction, showing that a little carbon was generated during the reaction. EDS analysis of the spots marked in Figure 8 showed the percentage of element Ni, Sn, C and O in table 2. Ni element was comprised of approximate 40%, which exceeded 1.5 times than approximate 18% of Sn element, reflected that Ni element was accumulated rich on the surface. Sn/O molar ratio was calculated to range in 1~1.5, confirmed that the mixture of SnO and SnO₂ were existed over the surface of oxidized Ni₃Sn₂ after reaction. The detected C had approximate 18~22% , which was supposed to come from the C deposited on the surface of the particles during methanol decomposition.

The experimental results show that oxidized Ni₃Sn₂ exhibits much higher degree of catalytic activity for decomposing methanol than that of Ni₃Sn₂ in the temperature range of 320~360 °C. This catalytic behavior was supposed to be related to the Ni₃SnO₂ serving as the active species for decomposing methanol, combined with the results of catalytic test, XRD, TPR and SEM. The similar phenomenon was also observed by A. C. Grijalba and A. Neramittagapong [10, 11]. The oxidized Ni₃Sn₂ began to have catalytic activity from 320 °C at which the reduction of NiO→Ni occurred. The activity increased as more Ni amount generated with increasing temperature. When the temperature was up to 360 °C, the activity began to decrease with increasing temperature at which the reduction of SnO₂→SnO occurred. The activity continued to decrease with increasing temperature as more SnO₂ amount was reduced. The Ni₃SnO₂ catalyst is greatly advantageous for producing H₂ from decomposing methanol, as it significantly decreased the methanation and water-gas shift which decreased the efficiency of H₂ production.

4. CONCLUSIONS

The catalytic properties of oxidized Ni₃Sn₂ were investigated for decomposing methanol in the range 240–480 °C, and the following results were obtained:

- 1) The oxidized Ni₃Sn₂ showed high degrees of catalytic activity for decomposing methanol and suppressed methanation

Table 2. EDS results of oxidized Ni₃Sn₂ after 28 h of reaction at 320 °C.

Spot No	Ni(at%)	Sn(at%)	C(at%)	O(at%)	O/Sn
1	43.6	17.5	18.6	18.3	1.1
2	37.9	17.3	20.9	23.9	1.4
3	39.1	17.4	18.6	24.9	1.4
4	40.9	17.7	19.3	22.1	1.3
5	38.9	17.8	21.6	22.7	1.3
6	38.7	17.6	20.8	22.9	1.3
7	40.2	18.4	18.3	23.1	1.3
8	40.3	18.6	19.2	21.9	1.2
9	39.9	18.0	19.4	22.7	1.3

and water-gas shift reaction over the whole temperature range tested.

- 2) The oxidized Ni₃Sn₂ was spontaneously activated in the temperature range of 320~360 °C and deactivated with increasing temperature from 360 to 480 °C. From the results of XRD, SEM, TPR, etc, the reduction of NiO→Ni improved the activity of oxidized Ni₃Sn₂ but the reduction of SnO₂→SnO decreased the activity of oxidized Ni₃Sn₂. Therefore, the Ni₃SnO₂ catalyst was considered as the active sites.
- 3) The Ni₃SnO₂ catalyst is greatly advantageous for producing H₂ from decomposing methanol as it has low methanol decomposition temperature, low cost and high efficiency of H₂ production. Therefore, it maybe a potential catalyst for hydrogen production from methanol.

5. ACKNOWLEDGMENTS

This work was financially supported by research fund of key laboratory for advanced technology in environmental projection of Jiangsu province and Guangxi Key Laboratory of Information Materials (Guilin University of Electronic Technology), China (Project No. 1210908-02-K).

REFERENCE

- [1] A. Penkova, L. Bobadilla, S. Ivanova, M.I. Dominguez, F. Romero-sarria, A.C. Roger, M.S. Centeno, J.A. Odriozola, *Applied Catalysis A:General*, 392, 184 (2011).
- [2] S. Saadi, B. Hinnemann, S. Helveg, C.C. Appel, F. Abild-Pedersen, J.K. Nørskov, *Surface Science*, 603, 762 (2009).
- [3] C. Padeste, D.L. Trimm, R.N. Lamb, *Catalysis Letters*, 17, 333 (1993).
- [4] E. Nikolla, J. Schwank, S. Linic, *J. Catal.*, 263, 220 (2009).
- [5] J.W. Shabaker, G.W. Huber, J.A. Dumesic, *J. Catalysis*, 222, 180 (2004).
- [6] A. Onda, T. Komatsu, T. Yashima, *Phys. Chem. Chem. Phys.*, 2, 2999 (2000).
- [7] S.D. Robertson, B.D. McNicol, J.H. Baas, S.C. Kloet, *J. Catalysis*, 37, 424 (1975).
- [8] J.S Lee, J. Kim, M. Kang, *Korean Chem. SOC.*, 32, 1912 (2011).
- [9] Q. Zhao, H. Lorenz, S. Turner, O.I. Lebedev, G.V. Tendeloo, C. Rameshan, S. Penner, *Applied Catalysis A:General*, 375, 188 (2010).
- [10] A.C. Grijalba, J. Urresta, A. Ramirez, J. Barrault, J. the Argentine Chemical Society, 98, 48 (2011).
- [11] A. Neramittagapong, N. Grisdanurak, S. Neramittagapong, *J. Industrial and Engineering Chemistry*, 14, 429 (2008).